Distinct structural patterns of the human brain: A caveat for registration

Frithjof Kruggel

Department of Biomedical Engineering, University of California, Irvine, USA
fkruggel@uci.edu, http://sip.eng.uci.edu

Abstract. Current approaches for analyzing structural patterns of the human brain often implicitly assume that brains are variants of a single type, and use nonlinear registration to reduce the inter-individual variability. This assumption is challenged here. Regional anatomical and connection patterns cluster into statistically distinct types. An advanced analysis proposed here leads to a deeper understanding of the governing principles of cortical variability.

Keywords: structural patterns · connectivity · human cortex.

1 Introduction

Cortical structures of the human brain show a puzzling complexity and inter-individual variability. Numerous analytic approaches implicitly assume that structural properties of brains, represented in any high-dimensional space, form a single cluster and use nonlinear registration to reduce the inter-individual variability. We challenge this assumption. Depending on the features and similarity criteria involved in the registration process, the total variance is reduced by only 20-40%. Consider a simplifying analogy: Suppose we want to study structural properties of cars. We hardly doubt that a registration procedure can be designed that successfully matches gross car parts (e.g., the passenger and engine compartment, the trunk and wheels). However, when zooming into details, objects under study become distinct (e.g. a trunk of a truck vs. a sports car, a combustion engine vs. an electric motor). Here, we demonstrate here that structural variants of brain regions with distinctive properties exist in a population. Avoiding an arguable registration and embracing the actual variability leads to analytic procedures that actually *explain* sources of variability at a considerably larger proportion.

2 Methods

Data source: We used anatomical and diffusion-weighted MRI data acquired in $nc = 1061$ subjects of the publicly available Human Connectome Project [2]. *Anatomical processing:* We started out from triangulated meshes representing the white-gray matter interface of a hemisphere with a topological genus

of zero. Using local curvature and geodesic depth, the surface was segmented into patches called *basins* that were centered around a locally deepest point, the *sulcal root*. A most isometric mapping was used to transfer and re-parameterize vertex-wise properties (e.g., basin label, depth, curvature) onto a common sphere with $nv = 163842$ vertices. Thus, we represented structural information as an image of $nc \times nv \times np$ properties. Refer to [4] for details. *Tractography:* Diffusion-weighted data were corrected for subject motion and susceptibility distortions. Voxel-wise estimates of the orientation distribution function of water mobility were computed using the constrained spherical deconvolution method [3]. Probabilistic tracking [5] from basin-labeled surface seeds was performed to determine connectivity between basins. Results were kept in hemisphere-wise connectivity matrices C, where each element $C(i,j)$ corresponded to the probability of connecting basin i to j. Thus, C can be regarded as a discrete, empirical PDF of basin connectivity. *Distance metrics:* We computed a co-occurence matrix M of the basin labeling in hemispheres a, b and expressed the their structural distance by $D_M = 1 - \mathrm{NMI}(M_{a,b})$. For connectivity, we selected the Hellinger distance metric by experimentation:

$$\mathrm{D_C}(a,b) = \sqrt{2\left(1 - \sqrt{2\sum_i \sum_j \sqrt{C_a(i,j)\, C_b(i,j)}}\right)}. \tag{1}$$

Statistical assessment: We computed the distance metrics for all hemisphere pairs a, b and compiled them in matrices for structure D_M and connectivity D_C of dimensions $nc \times nc$. Both matrices were mapped into a low-dimensional space using the ISOMAP algorithm [6], with a target dimension of $nd = 4$ estimated by the Grassberger-Procaccia method [1]. Thus, structural and connectivity of a hemisphere were represented by a point in an 8-dimensional space. We used a Gaussian mixture model to cluster into groups, where the number of classes was determined from the maximal Bayesian information criterion and silhouette coefficient. Note that this analysis can be restricted to any sub-region of the whole hemisphere.

3 Results

Due to space limitations, we provided results for the central sulcus (CS) only. For each dimension of the structural and connectivity matrices, we analyzed their dependence on several variables using linear regression (Tab. 1). Dimensions and their amount of represented variance were compiled in the second column. The first dimension represented more than 50% of the variance, and corresponded to the "regularity" of the sulcus structure. Regular sulci were straight, deep, and consisted of relatively few basins, in contrast to tortuous, shallow sulci with a larger number of basins (Fig. 1). Considering the number of basins as a proxy for structural regularity, we found that between 25% and 41% of the variance (R^2) were addressed to regularity. About 10% of the overall variance were explained by subject sex, handedness, and brain volume.

Table 1. Analysis of dimensions obtained from domain decomposition of distance matrices for the central sulcus on the left and right side. The relevance of dimensions 1-4 was assessed in relation to the number of basins in this sulcus, demographic variables sex, handedness, and heritability.

Model	Dimension		# of Basins			Brain Volume		Sex		Handedness		Heritability	
		exp.var.	p-value	code	R^2	p-value	code	p-value	code	p-value	code	p-value	code
Structure	1	0.559	< 2e-16	***	0.337	n.s.	–	n.s.	–	n.s.	–	n.s.	–
left	2	0.123	8.13e-4	***	0.026	1.95e-5	***	n.s.	–	n.s.	–	1.05e-4	***
	3	0.084	4.29e-6	***	0.037	5.51e-3	**	1.54e-3	**	0.0149	*	n.s.	–
	4	0.045	< 2e-16	***	0.127	n.s.	–	n.s.	–	n.s.	–	n.s.	–
Structure	1	0.588	< 2e-16	***	0.255	n.s.	–	n.s.	–	0.0413	*	n.s.	–
right	2	0.098	0.0170	*	0.038	2.48e-8	***	1.13e-4	**	n.s.	–	0.0349	*
	3	0.058	1.49e-13	***	0.054	0.016	*	n.s.	–	n.s.	–	n.s.	–
	4	0.046	< 2e-16	***	0.194	n.s.	–	n.s.	–	n.s.	–	n.s.	–
Connectivity	1	0.562	< 2e-16	***	0.406	n.s.	–	7.40e-3	**	n.s.	–	n.s.	–
left	2	0.230	< 2e-16	***	0.139	n.s.	–	n.s.	–	n.s.	–	4.44e-3	**
	3	0.106	0.0378	*	0.020	2-69e-3	**	8.35e-3	**	6.29e-3	**	n.s.	–
	4	0.030	n.s.	–	0.024	5.45e-5	***	n.s.	–	n.s.	–	0.0451	*
Connectivity	1	0.528	< 2e-16	***	0.380	n.s.	–	n.s.	–	n.s.	–	n.s.	–
right	2	0.253	< 2e-16	***	0.111	n.s.	–	n.s.	–	n.s.	–	n.s.	–
	3	0.119	1.52e-5	***	0.025	n.s.	–	0.0122	*	n.s.	–	n.s.	–

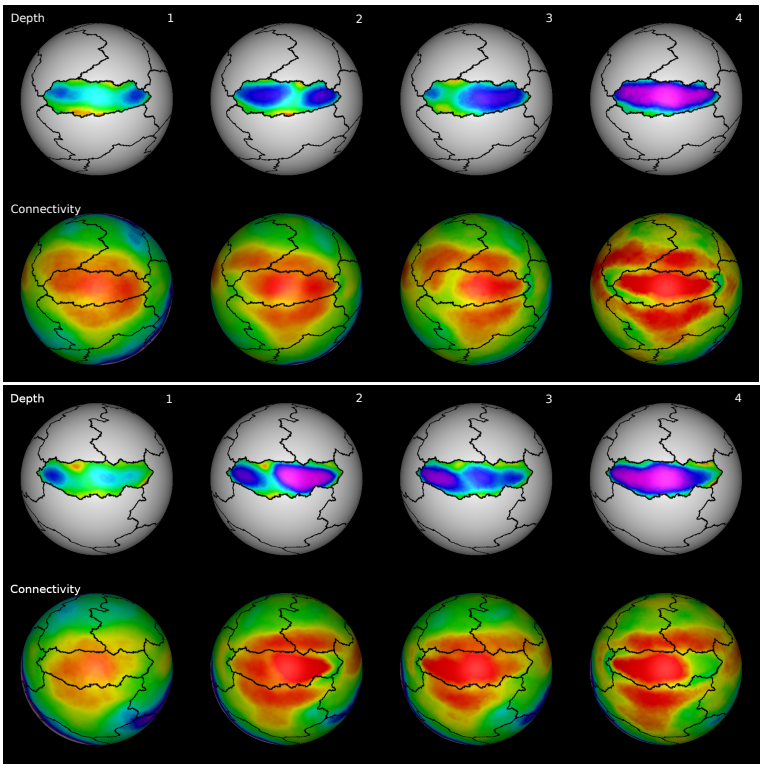

Fig. 1. Clustering of the central sulcus (CS) into four distinct, mirror-symmetric configurations on the left (top) and right (below) side. Rows 1, 3 show geodesic depth (increasing from red to magenta). Rows 2, 4 show the connection strength (increasing from magenta to red).

Significant influences of subject sex, handedness, and brain volume were typically found for the second structural dimension and the third connectivity dimension. We assessed the absolute difference of scores within subject pairs grouped by genetic similarity. This heritability was typically reflected in the second dimension, representing between 2% and 6% of the total variance.

Clustering yielded four distinct structural and connectivity patterns (Fig. 1), with mirror-symmetric patterns on the left (top panel) and right side (below). Patterns were sorted by increasing regularity from left to right, as determined from scores of the first dimension above. The first pattern (column 1) showed a low regularity, consisting of two shallow centers of low variability. Patterns 2 and 3 revealed two stronger centers, in pattern 2 more prominent in the upper CS, in pattern 3 more prominent in the lower CS. Finally, pattern 4 showed a straight and deep sulcus with high regularity. Interestingly, more regular sulcal patterns were related to a stronger, more distinctive connectivity (rows 2 and 4). Note that connection strength closely followed a lower basin variability not only in the central sulcus, but also adjacent regions in the pre- and post-central sulcus, and the mid-posterior insula on both sides.

4 Conclusion

By this short demonstration, we wanted to illustrate two points: (1) Structural and connectivity patterns of the human brain do not originate from a continuum, but show distinct properties, at least at the regional level. This finding renders the application of registration processes as arguable, at least at the hemispheric level. (2) Instead of attempting to reduce the inter-individual variability by registration, we suggest to embrace this variability and to analyze and identify their sources. As demonstrated here, up to 80% of the total variance can be explained by identifiable factors.

References

1. Grassberger P., Procaccia I.: Characterization of strange attractors. Physica D: Nonlinear Phenomena 9, 189–208 (1983)
2. Human Connectome Project: 1200 Subjects Data Release Reference Manual. https://www.humanconnectome.org/study/hcp-young-adult/document/1200-subjects-data-release. accessed: April 17, 2022
3. Jeurissen B., Tournier J.D., Dhollander T., Connelly A., Sijbers J.: Multi-tissue constrained spherical deconvolution for improved analysis of multi-shell diffusion MRI data. NeuroImage 103, 411–426 (2014)
4. Kruggel F.: The macro-structural variability of the human neocortex. NeuroImage 172, 620–630 (2018)
5. Smith R.E., Tournier J.D., Calamante F., Connelly A., Anatomically-constrained tractography: improved diffusion MRI streamlines tractography through effective use of anatomical information. NeuroImage 62, 1924–1938 (2016)
6. Tenenbaum J.B., de Silva V., Langford J.C.: A global geometric framework for nonlinear dimensionality reduction. Science 290, 2319–2323 (2000)